Available online at www.sciencedirect.com
ScienceDirect
Polymer 48 (2007) 5917–5927
polymer
www.elsevier.com/locate/polymer

Phase continuity detection and phase inversion phenomena in immiscible polypropylene/polystyrene blends with different viscosity ratios

T.S. Omonov [a,1], C. Harrats [b,2], P. Moldenaers [a,*], G. Groeninckx [b,**]

[a] *Katholieke Universiteit Leuven, Department of Chemical Engineering, Division of Applied Rheology and Polymer Processing, Willem de Croylaan 46, 3001 Leuven, Belgium*

[b] *Katholieke Universiteit Leuven, Department of Chemistry, Division of Molecular and Nanomaterials, Laboratory of Macromolecular Structural Chemistry, Celestijnenlaan 200 F, 3001 Leuven, Belgium*

Received 21 June 2007; received in revised form 1 August 2007; accepted 4 August 2007
Available online 9 August 2007

Abstract

Blends of polypropylene (PP) and polystyrene (PS) were prepared in a twin-screw extruder and studied in a wide range of compositions. Phase continuity was first determined using selective solvent extraction. Subsequently, dynamic stress rheometry and dynamic mechanical analysis were used to detect the co-continuity and phase inversion compositions in the melt and the solid states. It appears that the phase inversion occurs in a domain rather than at a single point. The evaluation of the storage modulus of PP/PS blends in the melt at a constant low frequency gives information about the co-continuity, as far as the onset of co-continuity and phase inversion composition of the PS phase are concerned. The evaluation of the storage modulus and mechanical loss factor at a constant high temperature, or the glass transition temperature intensity allowed to precisely detect the phase inversion composition. The fractionated or bulk crystallization behavior of the crystallizable PP phase in the PP/PS blends can also be used to identify the matrix/dispersed phase or co-continuous phase morphology. Several semi-empirical models using the dynamic viscoelastic properties of blend components have been applied to detect the phase inversion composition. An extensive data set presented, can also be used to guide future modeling.

Keywords: Polypropylene/polystyrene blends; Co-continuity; Phase inversion

1. Introduction

It was long believed that co-continuous phase morphologies are mainly formed closely near the point of phase inversion. Recently, several authors have shown that co-continuous structures can be formed in a domain of compositions rather than at a single point [1–10] and, the formation of co-continuous morphologies, especially at low concentrations, is due to the existence of elongated and interconnected network structures [11,12].

Co-continuous phase morphologies in polymer blends can be developed at initial, intermediate and final stages of the blending depending on mixing conditions, interfacial emulsifiers and the type of blenders/extruders used [13–19]. There are some discussions in the literature as to whether the formation of the phase morphology in polymer blends proceeds via the droplet deformation/breakup mechanism [20,21] or by a sheet forming mechanism [22,23].

A wide range of techniques have been described in the literature to detect the co-continuity. The most classical method is the solvent extraction procedure, which allows to quantify the phase continuity on a 3D scale. This method is widely employed and examples for quantification of the co-continuity degree are given in the literature [24–31]. The success of

* Corresponding author. Tel.: +32 16 32 23 59; fax: +32 16 32 29 91.
** Corresponding author. Tel.: +32 16 32 74 40; fax: +32 16 32 79 90.
E-mail addresses: paula.moldenaers@cit.kuleuven.be (P. Moldenaers), gabriel.groeninckx@chem.kuleuven.be (G. Groeninckx).
[1] Tel.: +32 16 32 23 59; fax: +32 16 32 29 91.
[2] Tel.: +32 16 32 74 40; fax: +32 16 32 79 90.

0032-3861/$ - see front matter © 2007 Elsevier Ltd. All rights reserved.
doi:10.1016/j.polymer.2007.08.012

this technique depends on the existence of a couple of selective solvents; each solvent should be able to dissolve one phase without any influence on the other phase. In spite of the simplicity of this method, it has some drawbacks. Indeed, two phase systems have rarely two selective solvents and one component is often more solvent-resistant than the other. Moreover, in some cases, the application of the solvent extraction procedure may be destructive for the blends considered. Other popular methods are the use of different types of microscopic techniques, such as optical microscopy (OM) [27], scanning electron microscopy (SEM) [24–28,32,33], and transmission electron microscopy (TEM) [34–36]. These are often coupled with image analysis. However, an image is a two-dimensional (2D) object, and a fibrillar morphology can be viewed as droplets when the fibrils are observed perpendicularly to their axis. For this reason, it is suggested [36,37] to examine the collection of images from three orthogonal planes.

Rheological techniques can also help to determine the composition range of co-continuous phase morphologies in immiscible polymer blends. Indeed, it has repeatedly been shown that the droplet/matrix morphology displays a characteristic relaxation in the long time range. This leads to an enhancement of the elasticity, which can be observed in the storage modulus at low frequencies. This process is attributed to a shape relaxation of the deformed droplets, mainly driven by the interfacial tension [38–41]. Palierne model [42] perfectly fits this particular behavior. In contrast, the shape relaxation of co-continuous morphologies is less visible because of a reduced elasticity. Alternatively, several authors [43,44] have shown that the storage modulus of some polymer blends in the melt state follows a power law behavior in the terminal zone. Domains with different characteristic length scales entail a distribution of terminal relaxation times and a gel-like behavior. Vinckier and Laun [34] also used this feature to characterize the influence of time on the co-continuous morphology. They have followed the coarsening process by oscillatory measurements. It has been shown that the storage modulus decreases with time following the evaluation of the coarsening process of the co-continuous morphology. The co-continuous structure was considered as a network described by the number of interconnections, as an alternative of a characteristic size. During the coarsening process, the number of interconnections decreases, while the amount of dispersed particles increases. The relaxation of the large dispersed domains occurs at very low frequencies and, in turn, the storage modulus decreases.

Many other studies have been carried out considering the different rheological behaviors between droplet/matrix and co-continuous morphologies [45–47]. For example, Galloway and Macosko [45] have used rheological techniques to detect the existence of co-continuous structures in a PEO/PS blend system. The elasticity seems to provide a sensitive way to assess the co-continuity in polymer blends. Indeed, when the storage modulus at low frequencies is plotted as a function of composition, two maxima seem to suggest the boundary of co-continuity.

Huitric et al. [46] have also found two maxima in the volume fraction dependence of the viscosity in a PE/PA12 blend. Near the boundaries of the co-continuity window, the viscosity reaches a maximum and decreases within the intermediate areas. On the other hand, Steinmann et al. [47] suggest that a more efficient rheological criterion is the maximum of the storage modulus at a constant frequency. They have found only one maximum which indicates the maximum of co-continuity and the phase inversion concentration for a PS/PMMA blend. Probably, such discrepancies should be related to the processing stage, which is a key parameter for the materials under investigation.

Dynamic mechanical thermal analysis can also be a useful method to distinguish between dispersed and co-continuous structures. In co-continuous structures, the temperature dependence of the storage modulus reflects a greater contribution of both components, whereas in dispersed structures, the blend modulus is dominated by the matrix component [48]. The relationship between the storage modulus or the mechanical loss factor ($\tan \delta$) and the blend composition can also determine the region of phase inversion and the existence of co-continuous structures, as shown by Dedecker and Groeninckx [9]. Significant changes in the storage modulus and $\tan \delta$ peak height were observed in the phase inversion region. This method is also sensitive to differences in the length scale of the co-continuous structure, which is a measure of the level of coarseness. This effect was clearly shown by Quintens et al. [49–51] in annealed PC/SAN blends under different annealing conditions. By increasing the annealing time, a significant increase in the plateau region between both glass transitions is observed, reflecting a greater contribution of the PC phase storage modulus due to its coarsened co-continuous network.

Differential scanning calorimetry (DSC) has also been used as a tool for phase co-continuity detection in binary SAN/polyamide 6 blends [52]. It has been shown that the blend with the finely dispersed crystallizable PA6 phase undergoes fractionated crystallization, whereas a co-continuous phase morphology exhibits crystallization at the bulk PA6 temperature value.

Several empirical and semi-empirical models have been developed over the last three decades to estimate the phase inversion composition in terms of material properties and processing conditions [24,36,53–63]. These models attempt to explain phase inversion phenomena; they have been tested for different polymer blend systems without leading to a universal rule. The process is not fully understood yet and other complementary studies are needed.

The objective of the present study is to determine the co-continuity window and phase inversion compositions in immiscible PP/PS blends having different viscosity ratios, by means of different techniques. Solvent extraction is considered as the most direct technique and taken as a reference method to characterize the phase morphologies. Subsequently, the blends have been studied using dynamic stress rheometry (DSR), dynamic mechanical spectroscopy (DMTA) and DSC, in the melt and solid states. Several semi-empirical models using the dynamic viscoelastic properties have been applied.

2. Experimental

2.1. Materials

The pure polymers used in the present investigation were two different commercial polypropylene grades from BOREALIS having low and medium viscosities, and three different polystyrenes from BASF, POLYSTYROL R28/27, 143E and 158K having low, medium and high viscosities, respectively (Table 1).

2.2. Blend preparation

The blends were prepared by means of a twin-screw mini-extruder manufactured by DSM Research (The Netherlands). It consists of a mixing chamber with a capacity of 15 cm^3 and two co-rotating conical screws. By means of a re-circulation channel within the mixing chamber and a valve to open the mixing chamber, the residence time can be varied. Mixing was carried out under nitrogen flow to prevent thermal oxidation during compounding. All the blends were prepared according to the same experimental procedure. The mixing temperature was fixed at 215 °C. The PP and PS homopolymers are fed into the extruder after dry blending and the melt blending was carried out at a screw rotation speed of 100 rpm and was continued for 10 min.

2.3. Solvent extraction

To determine the composition window where the blends exhibit a droplet-in-matrix phase morphology or where the two phases are co-continuous, samples of known weight of each blend were stirred in chloroform for 7 days at a temperature of 50 °C to selectively extract the PS phase. Note that shorter times may be sufficient but that depends on the composition. Knowing that the continuity index of the blend depends on the sample thickness of the extracted blend [64], the samples for the selective extraction have been prepared from the strands of the blends with a thickness of 2–3 mm and a weight of 20–40 mg. The continuity index of the PS phase (CI_{PS}) was quantified as the percentage of the polystyrene phase that was extracted using Eq. (1):

$$CI_{PS} = \frac{m_{ini} - m_{ext}}{m_{ini}} \times 100\% \quad (1)$$

Table 1
Specifications of the blend components used

Homopolymer	η^* [Pa s] at 205 °C, 100 rad/s	Material code[a]	Supplier
PP37	260	PP_L	Borealis
PP6.5	613	PP_M	Borealis
PS R28/27	185	PS_L	BASF
PS 143E	603	PS_M	BASF
PS 158K	863	PS_H	BASF

[a] Note that the L, M and H indexes in the table denote the viscosities of homopolymers as low, medium and high.

where m_{ini} is the weight of the PS phase initially present in the blend and m_{ext} the weight of the PS phase in the blend after solvent extraction. In the case where the sample is not disintegrated, the polypropylene phase is considered as 100% continuous, and the continuity of PS is quantified from the weight of extracted PS. If the sample disintegrates completely, then PP is considered as fully dispersed in the PS matrix and PS is considered as 100% continuous.

2.4. Rheology

The rheological characterization of the pure polymers was carried out on a stress controlled rheometer from Rheometric Scientific (DSR200) using cone-plate geometry. Samples with a diameter of 25 mm and a thickness of 1 mm were compression molded from the test material using a Collin press at a temperature of 205 °C. The measurements were performed at 205 °C under nitrogen atmosphere. The frequency was varied from 100 to 0.06 rad/s and the strain amplitude was kept small enough (5%) to ensure a linear viscoelastic response of the polymers. Fig. 1 represents the complex viscosities of

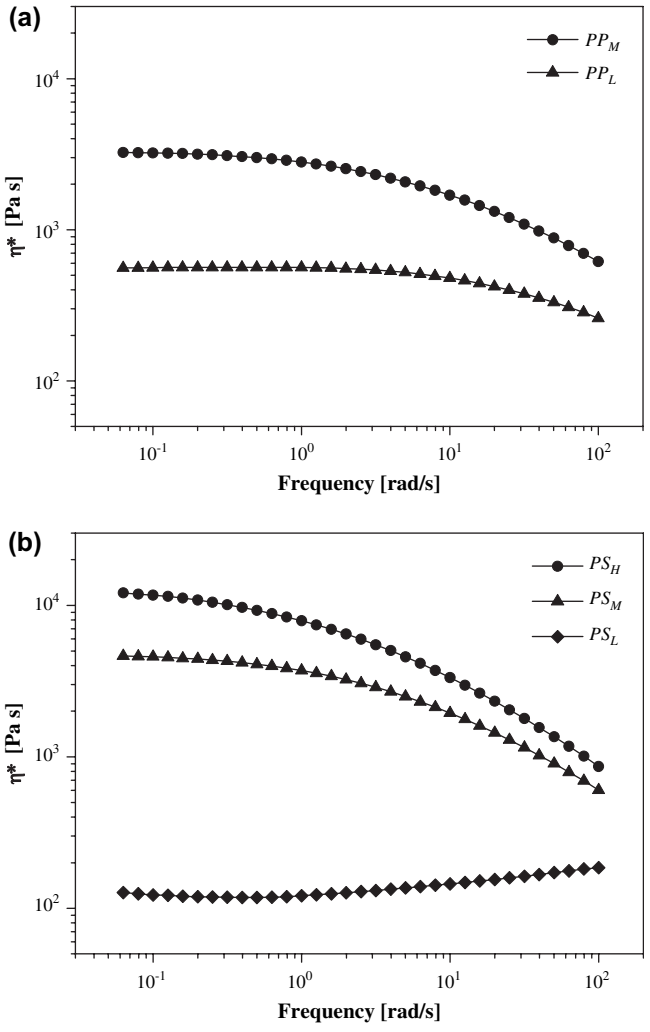

Fig. 1. Complex viscosities of various PP (a) and PS (b) homopolymers as a function of frequency at 205 °C.

PP (a) and PS (b) homopolymers as a function of frequency at a temperature of 205 °C.

2.5. Dynamic mechanical thermal analysis (DMTA)

The extruded polymer strands were compression molded in order to obtain bars ($60 \times 10 \times 4\ mm^3$) suitable for DMTA measurements. For this, the polymer strands were melted at 205 °C in a Collin press for 8 min; then, a pressure of 50 bar was applied. The melted samples were cooled down to room temperature under pressure. It has to be noted that the phase morphology of the molded samples is different from the as-extruded blends due to the structural instability, as reported in Ref. [12]. The dynamic mechanical properties were measured on a DMTA 2980 (TA instruments) in the dual cantilever mode at an oscillation frequency of 1 Hz. The sample was heated from −100 up to 150 °C at a heating rate of 3 K/min.

2.6. Differential scanning calorimetry

DSC measurements were performed using a DSC Pyris 1 series (Perkin–Elmer). The temperature and heat flow calibrations were performed using benzophenone ($T_m = 48.5$ °C), indium ($T_m = 156.6$ °C) and tin ($T_m = 231.88$ °C) at a heating and cooling rate of 10 K/min. Empty pan measurements were performed at the beginning of each series of tests. The sample was heated at a rate of 40 K/min to a temperature of 215 °C, where it was kept for 5 min to remove the thermal history. Then, the sample was cooled down at 10 °C/min to 25 °C. Subsequent melting scans were recorded at a heating rate of 10 K/min. In all the cases the sample weight was about 6 mg.

3. Results and discussion

3.1. Solvent extraction

In order to investigate the influence of the viscosity ratio on the blend phase morphology, three groups of PP/PS blends having different viscosity ratios have been prepared covering the whole blend composition range with steps of 10 wt%. The viscosity ratios of the components ranging from 0.3 to 3.3, at 100 rad/s and 205 °C, are summarized in Table 2. Note that the values of the shear viscosities of the PP and the PS components have been derived from their dynamic viscosities measured at a temperature of 205 °C and a frequency of 100 rad/s by applying Cox-Merz rule. The shear rate generated in the twin-screw mini-extruder using a screw rotation speed of 100 rpm has been approximated to 100 s^{-1} [65].

Table 2
Viscosity ratio of the components used at 100 rad/s and 205 °C

$\eta^*_{PS_L}/\eta^*_{PP_M}$	$\eta^*_{PS_M}/\eta^*_{PP_M}$	$\eta^*_{PS_H}/\eta^*_{PP_L}$
0.3	1.0	3.3

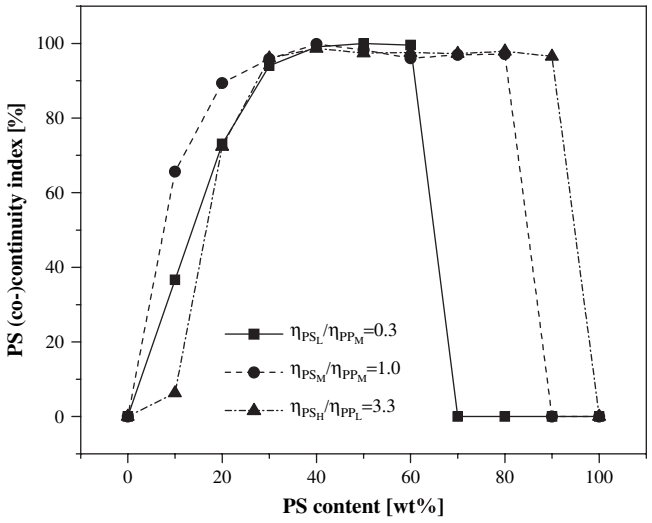

Fig. 2. PS phase (co-)continuity index as a function of PS phase content in the PP/PS blends having different viscosity ratios.

The continuity index of PS phase was determined from solvent extraction experiments and plotted as a function of the polystyrene content in the blends (Fig. 2). It is clear from Fig. 2 that the compositions at which the different blends exhibit full co-continuous phase morphologies cover a wide range of composition. The threshold of PS phase continuity depends on the viscosities of the PP and the PS phases. However, substantial differences between the blends are observed at the onset of PS phase continuity depending on the constituents used. The most effective mixing can be achieved under high shear when the viscosities of the blend components are equal [13]. In the equi-viscous blends ($\eta^*_{PS_M}/\eta^*_{PP_M} = 1$), the PS phase continuity threshold with a value of 66% at a composition of PP/PS 90/10 is observed. At this composition, the blend is composed of elongated fibrils and droplets of the PS phase. Note that the blends exhibit full co-continuity in the composition range from 30 to 80 wt% of PS. The phase morphology developed in PP/PS blends, studied by SEM, has been discussed in a previous paper [12].

The situation is different in the blends of high viscosity PS and low viscosity PP ($\eta^*_{PS_H}/\eta^*_{PP_L} = 3.3$). At composition of 90/10, low viscosity PP easily forms the matrix phase due to the minimized energy dissipation in the flow field [13]. Most of the PS forms dispersed particles in the PP matrix and only a small quantity of the PS is a part of a co-continuous morphology. In order to develop the same extent of PS continuity as in the equi-viscous blend (at 90/10), the volume fraction of the higher viscosity PS component has to be increased to the same extent as the viscosities differ to maintain the connectivity of PS particles. For these blends, the PS phase continuity threshold with a value of 72% is observed at a composition of 80/20 with the extent of full co-continuity range starting from 30 up to 90 wt% of PS.

In the blend composed of low viscosity PS and medium viscosity PP ($\eta^*_{PS_L}/\eta^*_{PP_M} = 0.3$), the PS phase can easily be dispersed and forms an elongated fibril-like structure in the PP matrix. But this structure is not stable due to the break up

and retraction of thin elongated PS fibrils. In this combination, the PS continuity threshold of 37% is observed at a composition of PP/PS 90/10. The full continuity range of PS in these blends is quite narrow within 30–60 wt% PS phase. The samples with compositions of 30/70, 20/80 and 10/90 PP/PS are disintegrated in a selective solvent proving that the PP phase is mainly dispersed in the PS matrix.

In summary, it can be concluded that increasing the minor phase viscosity (or decreasing the major phase viscosity) leads to less stable filaments of the minor phase, and co-continuity is possible at higher volume fractions or leads to a higher value of co-continuity threshold at fixed composition.

3.2. Melt-state dynamic mechanical spectroscopy: DSR

The purpose of the rheological measurements was to identify blend properties that show a characteristic change when the phase morphology changes from dispersed to co-continuous. Based on the existence of shape relaxation for polymer blends at low frequencies, rheological data are expected to be sensitive to a change in morphology. As an example, Fig. 3 compares the storage modulus of pure PP and PS homopolymers, and equi-viscous ($\eta^*_{PS_M}/\eta^*_{PP_M} = 1$, at 100 rad/s) PP/PS blends at a temperature of 205 °C.

The curves in Fig. 3 highlight the well-known shape relaxation. The shear storage modulus (G') of all blends reveals an excess of elasticity with regard to the PP phase. This excess of elasticity is clearly visible in the low frequency zone for the 10/90, 20/80 and 30/70 PP/PS compositions. The blends show higher elasticity compared to both PP and PS homopolymers. This increase in G' can be attributed to the relaxation of the interface [45]. For a clearer view of the influence of the blend composition, and therefore the blend morphology, both the storage modulus G' and tan δ for the equi-viscous PP/PS blends are plotted in Fig. 4 as a function of PS content.

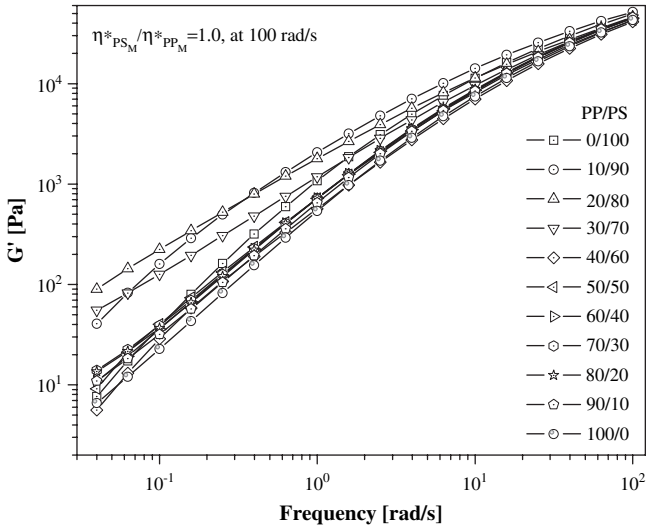

Fig. 3. Storage modulus (G') as a function of frequency for equi-viscous PP/PS blends at 100 rad/s and 205 °C (DSR).

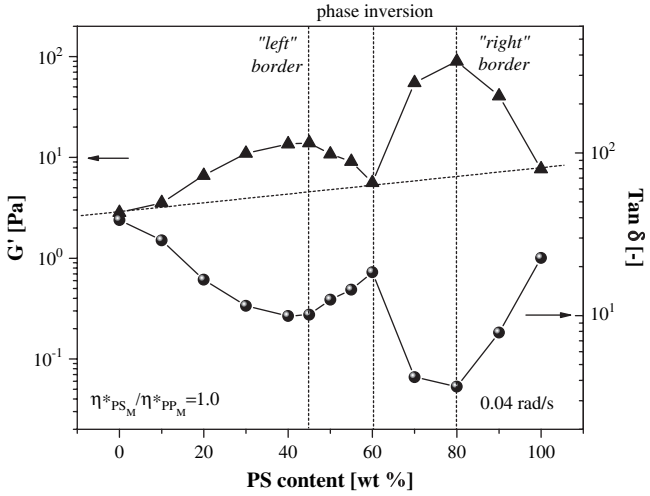

Fig. 4. Storage modulus (G') and tan δ as a function of PS content for equi-viscous PP/PS blends at 0.04 rad/s and 205 °C (DSR).

The composition dependence of the storage modulus G' reveals that it increases as the amount of PS phase increases, and reaches a maximum at a composition of PP/PS 55/45, drops in the middle of the composition window (at 60 wt% PS), then increases again reaching a maximum at a composition of PP/PS 20/80. The opposite behavior is seen, as expected, in the composition dependence of tan δ (bottom plot).

It is known that the elastic moduli of the blends can be modeled in a simple way considering the bulk contributions of the blend components and the contribution of the interface between the components [45]. The blends with a droplet/matrix morphology should display a higher interfacial area, and in turn an excess of elasticity [6], while a co-continuous phase morphology has a lower interfacial area.

The blend containing 10 wt% PS (see Fig. 4) has a dispersed/matrix phase morphology (in melt state [12]) with a certain amount of interface. An increase of the PS content causes an increase of the interfacial area (composition effect), while the contribution to the modulus from the components at a given composition remains constant. The elongated structures of the PS phase present in the PP matrix directly after extrusion at low PS content (see solvent extraction results) will break up into droplets due to the retraction and break up processes. This will cause an increase in the interfacial area (dispersion effect). It is obvious that a maximum area of the interface can be expected in blends having a dispersed/matrix phase morphology at a higher amount of PS (45 wt%); in other words, at a (‘‘left’’) border of co-continuity before the percolation of the dispersed PS particles occurs (Fig. 4). A further increase of the PS content in the blends leads to the formation of a co-continuous phase morphology: the interfacial area decreases dramatically and G' reaches a minimum value (40/60 PP/PS). The minimum area of the interface can be expected in blends having full co-continuous, interpenetrated phase morphologies. The minimum in the interfacial area can be considered as a phase inversion composition. This point is comparable with the values which result from the additivity

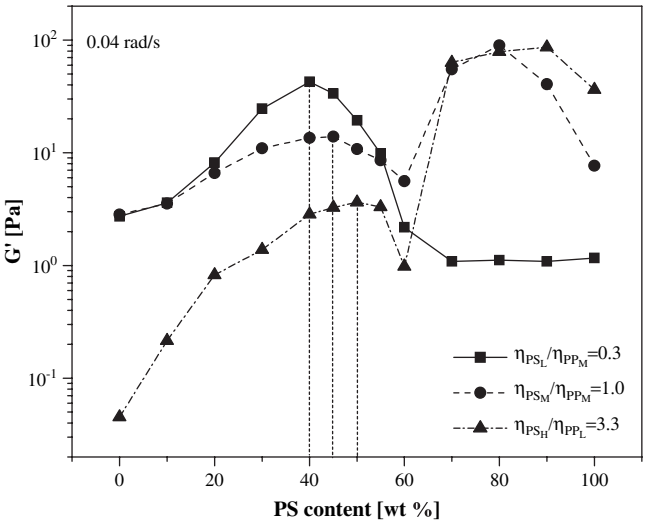

Fig. 5. Storage modulus (G') as a function of PS content for PP/PS blend groups having different viscosity ratio at 0.04 rad/s and 205 °C (DSR).

rules of elasticity of homopolymers (see dashed line in Fig. 4). A subsequent increase of the PS content in the blends leads to the formation of a PS matrix with a dispersed PP phase. At a composition of 20/80 PP/PS, PP is fully dispersed in the PS matrix with maximum available interface, and this composition can be considered as a threshold (or ''right'' border) of PP phase continuity.

Thus, the maximum of G' (or minimum of tan δ) at 45 wt% PS corresponds to the onset of the PS phase continuity, while another maximum at 80 wt% PS can be attributed to the threshold of PP phase continuity. These results suggest clearly that co-continuous morphologies exist for the equi-viscous PP/PS blends, in the range of 45–80 wt% of PS, with the phase inversion composition at 60 wt% PS, which is in good agreement with the results found in the literature [45].

Figs. 3 and 4 represented an example of the relaxation behavior of PP/PS blends with equal component viscosities. Fig. 5 represents the composition dependence of the storage moduli of three PP/PS blends having a different viscosity ratio. Note that the frequency dependence of G' for the non-equi-viscous blends (not shown here) shows the same trend as for the equi-viscous blends.

Based on the solvent extraction measurements, the blends with the lowest viscosity ratio ($\eta^*_{PS_L}/\eta^*_{PP_M} = 0.3$) have a maximum interfacial area (onset of PS phase continuity) at 40 wt% PS phase content, when PP is the matrix phase. In a group of blends with the highest viscosity ratio ($\eta^*_{PS_H}/\eta^*_{PP_L} = 3.3$), the threshold of PS continuity can be found at 50 wt% of PS phase (see dashed vertical lines). The phase inversion composition, as determined in the rheological measurements, does not seem to be very sensitive to the change of the viscosity ratio of the components compared with DMTA experiments (see Section 3.3). In all combinations of the viscosity ratio, the phase inversion composition appears at about 60 wt% of PS. It should be noted that due to the very low viscosity of PS_L, in a blend group with $\eta^*_{PS_L}/\eta^*_{PP_M} = 0.3$, it was too difficult to estimate the ''right'' border of continuity.

3.3. Solid-state dynamic mechanical spectroscopy: DMTA

As dynamic mechanical properties depend mainly on the nature of the matrix polymer, the results of the dynamic mechanical thermal analysis should also be sensitive to the change of the phase structure from dispersed/matrix to co-continuous and vice versa. The dynamic mechanical properties in the solid state were analyzed for all blend series of PP/PS over the whole composition range. The storage moduli (E') and the mechanical loss factor (tan δ) of pure PP, PS and PP/PS blends were measured from −100 to +150 °C at a heating rate of 3 K/min with a DMTA 2980 (TA instruments), using rectangular specimens in the dual cantilever mode, are shown in Figs. 6 and 7 for the equi-viscous blends.

It can be seen that at low temperatures the values of E' of the PP phase are higher than those of the PS phase. As

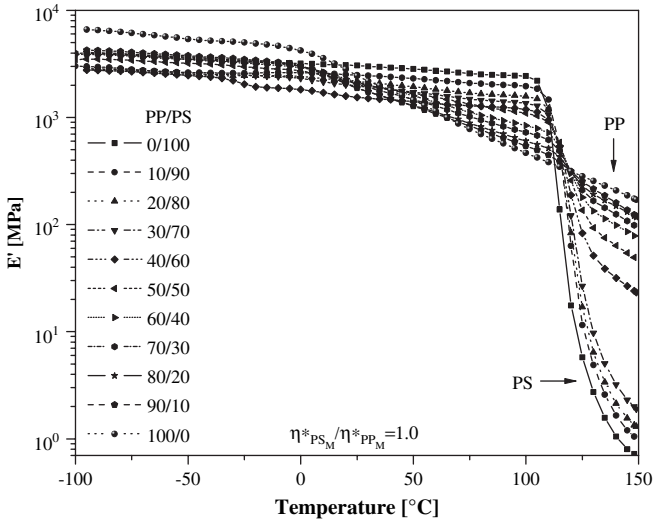

Fig. 6. Storage modulus (E') as a function of temperature for equi-viscous PP/PS blends at a frequency of 1 Hz (DMTA).

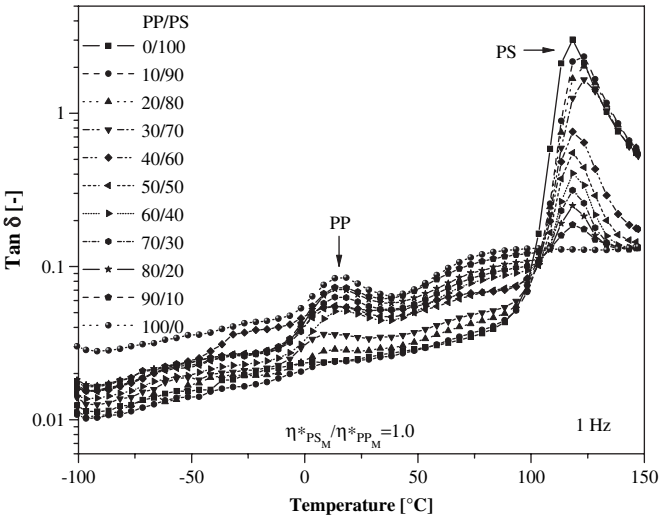

Fig. 7. Tan δ as a function of temperature for equi-viscous PP/PS blends at a frequency of 1 Hz (DMTA).

expected, the E' drops upon increasing the temperature due to the increased segmental mobility. In semicrystalline polymers like PP, only the amorphous part undergoes segmental motion, while the crystalline part remains in the solid state until the melting temperature is reached. The glass transition temperature (T_g) of PP is about 10 °C, and after this temperature the slight linear decrease of the storage modulus of PP is observed. Polystyrene is fully amorphous and its storage modulus does not change much upon increasing the temperature until the T_g is attained.

The rapid decrease of E' in PS and PP/PS blends around 120 °C corresponds to the T_g of the amorphous polystyrene. As expected, incorporation of PS into the PP matrix results in a remarkable increase in stiffness of the PP/PS blends. The E' vs. T curves of the PP/PS blends show an enhanced rubbery plateau, indicating the reinforcement effect. On increasing the temperature, the drop in E' of the PP phase is compensated by the stiffness of the PS phase.

The analysis of the temperature dependence of tan δ (Fig. 7) of PP shows that tan δ increases first, reaches a maximum at the glass transition temperature (at around 17 °C, the β transition), then decreases and again reaches a plateau region as a consequence of the α transition.

This α transition is due to the presence of "rigid" amorphous molecules present in the crystals [66,67]. The glass transition temperature (T_g) for the pure amorphous PS was found to be about 120 °C. This temperature position of T_g increases linearly up to 126 °C in PP/PS blends with a PS matrix and PP dispersed particles (before the phase inversion). The reason for this temperature shift is not clear yet. A further increase of the PP content in the PP/PS blends leads to a co-continuous phase morphology and the T_gs of the blend components appear in the same temperature position as for pure PS T_gs.

As can be seen from Figs. 6 and 7, the E' and tan δ of the PP/PS blends have wide-ranging values at high temperatures. In order to have a maximum contribution of the crystalline phase of PP to the E' and tan δ, a temperature of 150 °C was selected. The values of E' and tan δ at 150 °C are plotted as a function of the PS content in Fig. 8. Also the peak maximum of tan δ of the PS phase is shown in this figure. At this temperature, pure PP exhibits its solid-state properties because it is still below its melting point (163 °C, measured by DSC), and E' is relatively high (or the value of tan δ is low). However, at 150 °C, the amorphous PS phase is well above its T_g, and the storage modulus of PS is quite low allowing for maximum contribution from the PP phase as it is in the semicrystalline state (see points at 100 wt% PS).

By addition of PS (10–30 wt%) to PP, the modulus of PP/PS blends slightly decreases, but PP still remains as a matrix phase. Further increasing the PS content in the blends starting from 40 wt% leads to the formation of a co-continuous network structure due to the enhanced coalescence of PS particles. Phase inversion occurs between 60 and 70 wt% PS. At this point, the values of E' as well as tan δ are drastically changed (see dashed area in Fig. 8). The PS phase tends to form the matrix phase. In addition, it should be noted that the peak intensity of the T_gs of PP and PS phases in the blends is also sensitive to the change in

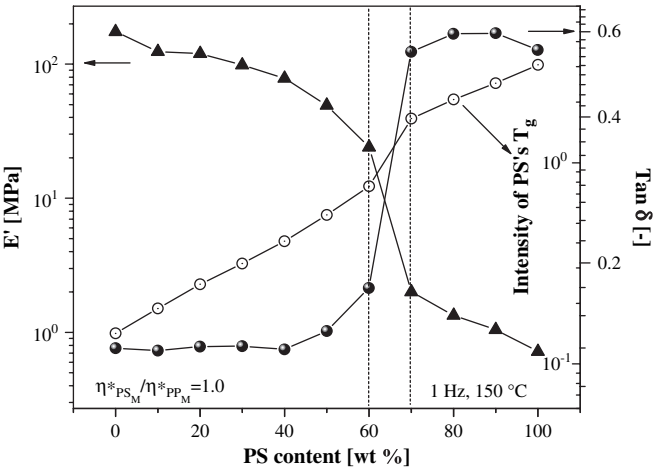

Fig. 8. Storage modulus (E'), tan δ and PS phase T_gs' intensity as a function of the PS concentration for equi-viscous PP/PS blends at a frequency of 1 Hz and a temperature of 150 °C (DMTA).

phase structure. The drastic change in the intensity of the T_g of the PS phase in the blends is an additional indication of the occurrence of phase inversion.

Fig. 9 compares the concentration dependence of tan δ at a temperature of 150 °C and an oscillation frequency of 1 Hz, for the homopolymers and blends having the three different viscosity ratios mentioned in Table 2. All the blend systems show the same trend for the phase inversion. The lowest composition at which the phase inversion occurs (40/60 wt% PP/PS) belongs to the blends with the smallest viscosity ratio (0.3). For the blends with the viscosity ratio of 3.3, the phase inversion occurs as high as 72 wt% of PS.

3.4. Differential scanning calorimetry (DSC)

It is now well known that the crystallization behavior of a crystallizable polymer dispersed in a matrix phase depends

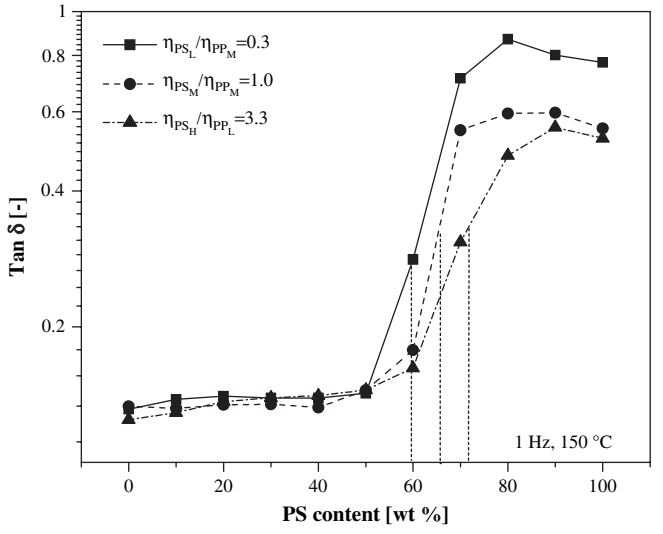

Fig. 9. Loss factor (tan δ) as a function of PS concentration for PP/PS blends with different viscosity ratios at a temperature of 150 °C and a frequency of 1 Hz (DMTA).

on the size of the particles. When the sample is composed of a matrix/droplet phase morphology, nucleation of the crystallizable polymer is restricted to the volume of the droplet. Each droplet will crystallize according to the number and type of heterogeneities present in it, or undergoes homogenous nucleation. If the particle size distribution of the dispersed component is broad, some fraction of the droplets can be nucleated by the heterogeneities they contain, whereas droplets that do not contain any heterogeneities (or are smaller than the size of a heterogeneity) can undergo homogenous nucleation at a larger degree of supercooling [68–71]. The blend system investigated here contain an amorphous PS and a crystallizable PP phase. Based on the fractionated crystallization approach, the boundary of continuity for the crystallizable PP phase can be established using DSC. As can be seen from Fig. 10, pure PS is amorphous and does not show any crystallization. The bulk crystallization temperature of neat crystallizable PP is 121 °C.

This bulk crystallization temperature of PP is not changed in the PP/PS blends within the composition range of PP/PS 100/0 to 40/60 wt%. Indeed, PP is fully co-continuous. A further increase of the PS content in the blends (e.g. 30/70 wt%) leads to the formation of a mixed phase morphology (see magnified part of Fig. 10a in Fig. 10b). At this composition a crystallization peak appears at 121 °C and another peak at 76 °C. The peak at 121 °C is attributed to the bulk crystallization of PP, whereas the second peak at lower temperature is due to homogenous nucleation of the PP droplets. The composition of 20/80 PP/PS has a broader size distribution. As a consequence fractionated crystallization peaks are obtained at 121, 103 and 76 °C. The blend having a composition of 10/90 PP/PS has only one peak at 76 °C due to the homogenous crystallization of small droplets of the PP phase in the PS matrix. Although it is not as accurate as solvent extraction and dynamic mechanical spectroscopy, the present DSC data can be used to distinguish the droplet/matrix and co-continuous phase structures. From the calorimetric measurements it can be concluded that the (“right”) boundary of continuity of the crystallizable PP phase in PP/PS blends is located at the composition of 30/70 wt% PP/PS.

3.5. Phase inversion composition and co-continuity prediction

Several empirical and semi-empirical models have been developed over the last three decades to estimate the phase inversion composition in terms of material properties and processing conditions, as they are empirical, they do obviously rely on experimental findings [24,36,53–63]. The idea of a simple relationship describing the phase inversion through the individual torque ratio of the blend components was first suggested by Avgeropoulus et al. [53,54]. Paul and Barlow [55] proposed a similar equation, where, instead of the torque ratio, the viscosity ratio was used (see Table 3). Later this relationship was supported by Jordhamo et al. [56] and Gergen et al. [57]. Further, the proposed equation was generalized by Miles and Zurek [58] using dynamic viscosity under mixing conditions for blends having largely different viscosities. Furthermore, Ho et al. [59], Kitayama et al. [60] and Everaert et al. [61] have modified the general equation by introducing a prefactor and/or an exponent to fit better the experimental results. Instead of using viscoelastic parameters, Metelkin and Blekht [62] were the first to introduce an empirical relationship to predict the phase inversion using a concept of capillary instabilities of individual layers. Utracki [37,63] developed another approach based on emulsion theory using “intrinsic viscosities” and maximum packing volume fractions ($[\eta]$ and ϕ_m), which is valid for the blends within the viscosity ratio range of $0.1 < \eta_1/\eta_2 < 10$.

Recently, Steinmann et al. [36] proposed an approach based on the assumption that the shape relaxation times of blend components meet in a maximum, at the phase inversion composition (or vice versa, the minimum of form factor defines the maximum of co-continuity, therefore the phase inversion concentration). These authors found a strong correlation between the viscosity and elasticity ratios, and a corresponding equation was given based on the viscosity ratio at a certain constant

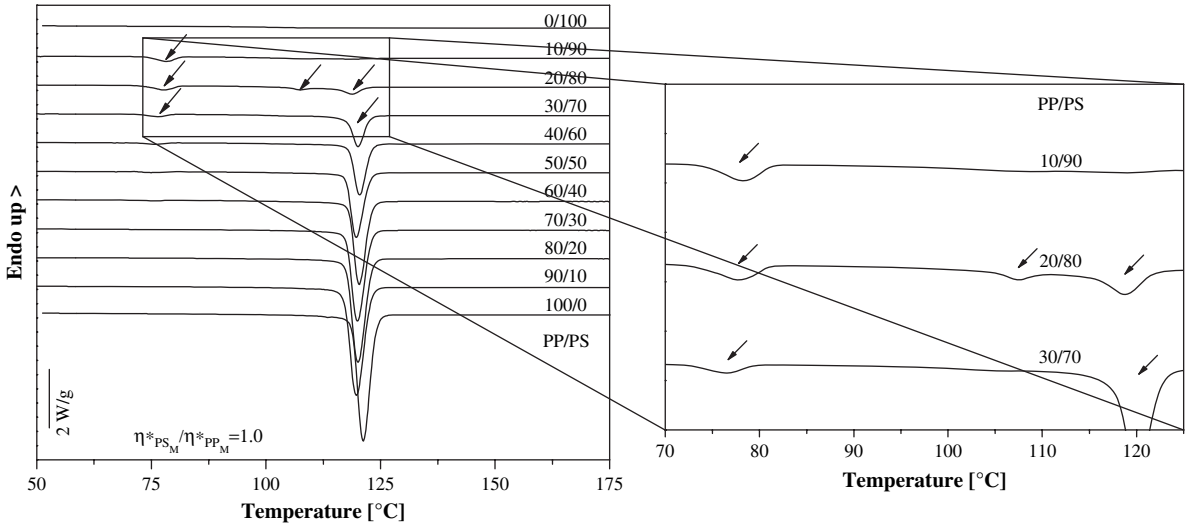

Fig. 10. DSC crystallization behavior of PP and equi-viscous PP/PS blends at a cooling rate of 10 °C/min.

Table 3
List of semi-empirical models and value of phase inversion compositions for PP/PS blends at different viscosity, elasticity and loss factor ratios, at 100 rad/s

References	Models	Phase inversion composition of PS [vol.%]		
		At η_{PS}/η_{PP}		
		0.3	1.0	3.3
Paul–Barlow [55], Jordhamo et al. [56], Gergen et al. [57], Miles–Zurek [58]	$\frac{\Phi_1}{\Phi_2} = \frac{\eta(\dot{\gamma})_1}{\eta(\dot{\gamma})_2}$	22	50	76
Ho et al. [59]	$\frac{\Phi_1}{\Phi_2} = 1.22\left[\frac{\eta(\dot{\gamma})_1}{\eta(\dot{\gamma})_2}\right]^{0.29}$	46	55	63
Kitayama et al. [60]	$\frac{\Phi_1}{\Phi_2} = 0.887\left[\frac{\eta(\dot{\gamma})_1}{\eta(\dot{\gamma})_2}\right]^{0.29}$	38	47	55
Everaert et al. [61]	$\frac{\Phi_1}{\Phi_2} = \left[\frac{\eta(\dot{\gamma})_1}{\eta(\dot{\gamma})_2}\right]^{0.3}$	41	50	58
Metelkin–Blekht [62]	$\Phi_2 = \left[1 + \frac{\eta_1}{\eta_2}\left[1 + 2.25\log\left(\frac{\eta_1}{\eta_2}\right) + 1.81\left(\log\left(\frac{\eta_1}{\eta_2}\right)\right)^2\right]\right]^{-1}$	8	49	89
Utracki [63]	$\Phi_2 = \frac{\left(1 - \log\left(\frac{\eta_1}{\eta_2}\right)/[\eta]\right)}{2},\ \eta = 1.9$	36	50	63
Steinmann et al. [36]	$\Phi_2 = -0.12\log\left(\frac{\eta_1}{\eta_2}\right) + 0.48$	45	52	58
		At G'_{PS}/G'_{PP}		
		0.05	1.1	4.6
Bourry–Favis [24]	$\frac{\Phi_1}{\Phi_2} = \frac{G'_2}{G'_1}$	5	48	18
		At $\tan\delta_{PP}/\tan\delta_{PS}$		
		0.12	1.2	2.3
Bourry–Favis [24]	$\frac{\Phi_1}{\Phi_2} = \frac{\tan\delta_1}{\tan\delta_2}$	11	45	30

elasticity. Bourry and Favis [24] have considered an elasticity contribution of the blend components and proposed a different approach using the storage modulus or loss factor ratios instead of viscosity ratios. The plots in Fig. 11 show a summary of empirical and semi-empirical models used for the prediction of the phase inversion composition and dual phase co-continuity of polymer blends as a function of the viscosity ratio in the range of 0.1–10. As can be seen these models

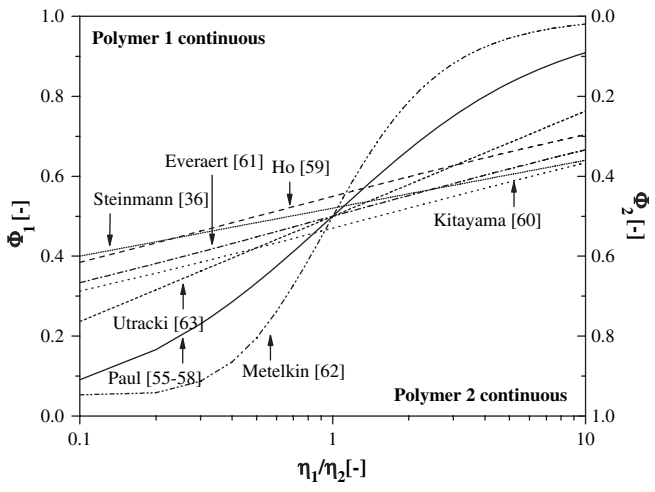

Fig. 11. Different semi-empirical models describing the phase inversion volume fraction as a function of the viscosity ratio of binary polymer blends.

attempted to predict the phase inversion, but the process is not fully understood yet, and there is a real need for other complementary studies.

Here, several models have been applied to PP/PS blend systems with different viscoelastic characteristics. The phase inversion compositions for all systems have been calculated using the above mentioned equations and the viscosities obtained at a shear rate of 100 rad/s. As we have seen from the solvent extraction results the full co-continuity of the PP/PS blends is within the range of 70/30 to 10/90 wt%, depending on the viscosity ratios of the constituents used. The results of melt-state mechanical spectroscopy showed similar results, where the blends have boundaries of continuity at compositions of 60/40 and 10/90 wt% PP/PS. It has been shown from solid-state mechanical spectroscopy that the boundaries of co-continuity are shifted to the highest PS content as the viscosity ratio is changed from 0.3 to 3.3. The phase inversion composition was not so sensitive to the change of the viscosity ratio in a melt-state rheological measurement. However, the solid-state mechanical measurements show a very clear influence of the viscosity ratio on the phase inversion composition. The results showed that the blends having a viscosity ratio $\eta^*_{PS_L}/\eta^*_{PP_M} = 0.3$ have a phase inversion composition at 60 wt% PS (see Fig. 9), whereas for the equi-viscous blends with $\eta^*_{PS_M}/\eta^*_{PP_M} = 1.0$, the phase inversion composition was obtained at 65 wt% PS. The blends having the highest value of the viscosity ratio ($\eta^*_{PS_H}/\eta^*_{PP_L} = 3.3$) have a phase inversion

composition at 72 wt% PS. It has to be mentioned that for the blends with a low and medium viscosity PS phase, the PS phase tends to be dispersed easily due to the minimum energy dissipation in the flow field [13], and the continuity threshold as well as the phase inversion composition can be reached at low concentration of PS. In the blend with the high viscosity PS, PS is coarsely dispersed and the percolation (as well as phase inversion) of the PS phase is delayed. The percolation of PS in this system will take place at a higher PS concentration than for a system where the viscosity ratio is unity or lower.

In order to compare the experimental results of the phase inversion composition, the weight percent values of the composition are converted to a volume fraction. Knowing the densities for the PP and PS homopolymers ($\rho_{PP} = 0.883$ g/cm^3, $\rho_{PS} = 1.05$ g/cm^3, respectively), one can easily get the volume fraction of the components which is 0.56, 0.61 and 0.67 for the viscosity ratios of 0.3, 1.0 and 3.3, respectively.

Fig. 12 represents the experimental points (obtained from solid-state dynamic mechanical analysis) as well as the fitting curves of the phase inversion composition (vol.%) as a function of the viscosity ratio for the different groups of PP/PS blends. The variation of the phase inversion volume fraction as a function of viscosity ratio, as obtained by fitting, will give an equation similar to that described in Refs. [59–61] with a different prefactor and exponent:

$$\frac{\Phi_1}{\Phi_2} = 1.59\left[\frac{\eta_1}{\eta_2}\right]^{0.19} \tag{2}$$

where Φ_1 and Φ_2 are the volume fractions, η_1 and η_2 represent the viscosity of PS and PP, respectively.

This model can also be used to detect the phase inversion composition, but the disadvantage of this model, as in the case of previous models, is that it does not take into account the requirements of the shape of the minor phase located in the matrix phase. Besides, other parameters like matrix viscosity, elasticity ratio or a combination of elasticity and viscosity may be considered. The problem is not simple because the full co-continuity of the blend system can be reached before (or after) the phase inversion composition, while this composition is an essential part of this phase co-continuity region. Finally, it seems that the geometry of the minor phase will play an essential role to define the percolation threshold and phase inversion composition, and even if their model is not predictive, the development of Willemse et al. [2,27] has to be considered. In order to ensure further progress in the understanding of the development of co-continuous morphologies, a combination of the different methods is required to precisely define the co-continuity window and the phase inversion composition in immiscible polymer blends.

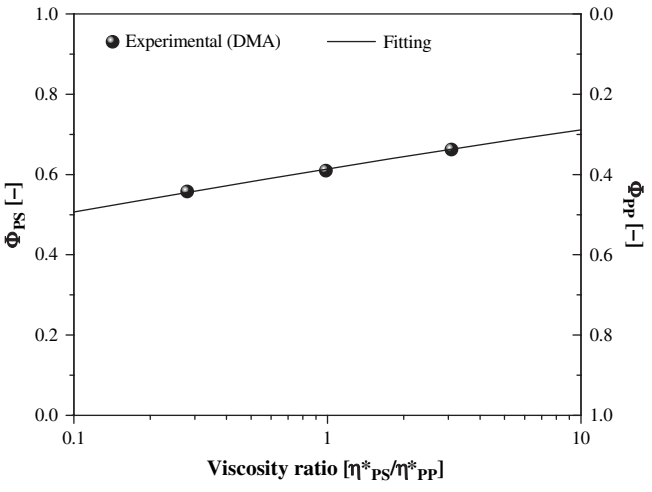

Fig. 12. Fitting of the experimental phase inversion volume fraction as a function of the viscosity ratio for PP/PS blends.

4. Conclusions

In this paper, a thorough characterization of the co-continuity domain and complex study of the phase inversion phenomena of PP/PS blends by means of different techniques were performed. The combination of different methods gives a clear picture of the phase morphology, as an addition to the morphological investigation reported in Ref. [12].

Selective dissolution experiments allowed to estimate quantitatively the window of PS phase full continuity for the several PP/PS blend systems studied, which is within the range of 70/30 to 10/90 wt%, depending on the viscosity ratio of the constituents used.

Melt-state rheological investigations using DSR show a clear difference between the dispersed/matrix and co-continuous structures, where the composition dependence of the shear storage modulus (G') of the blends shows local maxima at 60/40 and 10/90 wt% PP/PS. These maxima were attributed to the amount of interface present in these blends and described as boundaries of co-continuity. It has been shown that these boundaries are shifted to the highest PS content as the viscosity ratio is increased from 0.3 up to 3.3.

DMTA measurements of PP/PS blends have indicated that the tensile storage modulus (E') as well as tan δ show differences especially above the T_g of PS (at 150 °C). A blend with PS as a matrix shows a sharp decrease in E' whereas a co-continuous blend retains a higher modulus due to the greater contribution from the higher modulus of PP at this temperature. This method allows to detect precisely the phase inversion composition for the three different groups of PP/PS blends, which was 56, 61 and 67 vol.% for the viscosity ratios of 0.3, 1.0 and 3.3, respectively. Based on the experimental data of the phase inversion composition, an equation has been proposed to predict the phase inversion composition in immiscible polymer blends.

DSC measurements can also be used to distinguish crystallizable PP as dispersed phase or as a part of a co-continuous structure based on its fractionated crystallization behavior. If PP forms a dispersed phase, droplets of PP crystallize according to the number and type of heterogeneities present in it or undergo homogenous nucleation. If PP forms a co-continuous phase, normal bulk crystallization behavior is observed.

However, this method is limited to blend systems where the phases are able to show fractionated crystallization.

Acknowledgements

The authors are indebted to the Research Fund of the KULeuven for partial financial support in the framework of the GOA projects 98/06 and 03/06.

References

[1] Verhoogt H, Van Dam J, Posthuma de Boer A. Morphology-processing relationship in interpenetrating polymer blends. In: Klempner D, Sperling LH, Utracki LA, editors. Interpenetrating polymer networks. Advances in chemistry series, vol. 239. Washington; 1994. p. 333–51.
[2] Willemse RC, Posthuma de Boer A, van Dam J, Gotsis AD. Polymer 1998;39(24):5879–87.
[3] Willemse RC, Speijer A, Langeraar AE, Posthuma de Boer A. Polymer 1999;40(24):6645–50.
[4] Veenstra H, van Dam J, Posthuma de Boer A. Polymer 1999;40(5): 1119–30.
[5] Veenstra H, van Lent BJJ, van Dam J, Posthuma de Boer A. Polymer 1999;40(24):6661–72.
[6] Chaput S, Carrot C, Castro M, Prochazka F. Rheol Acta 2004;43(5): 417–26.
[7] Castro M, Carrot C, Prochazka F. Polymer 2004;45(12):4095–104.
[8] Li J, Favis BD. Polymer 2001;42(11):5047–53.
[9] Dedecker K, Groeninckx G. Polymer 1998;39(21):4993–5000.
[10] Harrats C, Mekhilef N. Co-continuous phase morphologies: predictions, generation and practical applications. In: Harrats C, Thomas S, Groeninckx G, editors. Micro- and nanostructured multiphase polymer blend systems: phase morphology and interfaces. FL, USA: CRC Press Taylor & Francis Group; 2006. p. 91–132 [chapter 3].
[11] Harrats C, Omonov TS, Groeninckx G, Moldenaers P. Polymer 2004; 45(24):8115–26.
[12] Omonov TS, Harrats C, Groeninckx G, Moldenaers P. Polymer 2007;48: 5298–302.
[13] Pötschke P, Paul DR. J Macromol Sci Part C Polym Rev 2003;C43(1): 87–141.
[14] Shih CK. Polym Eng Sci 1995;35(21):1688–94.
[15] Sundararaj U, Macosko CW, Shih CK. Polym Eng Sci 1996;36(13): 1769–81.
[16] Shih CK. Adv Polym Technol 1992;11(3):223–6.
[17] Shih CK, Tynan DG, Denelsbeck DA. Polym Eng Sci 1991;31(23): 1670–3.
[18] Lee JK, Han CD. Polymer 2000;41(5):1799–815.
[19] Lee JK, Han CD. Polymer 1999;40(23):6277–96.
[20] Taylor GI. Proc R Soc 1932;A138:41–8.
[21] Taylor GI. Proc R Soc 1934;A146:501–23.
[22] Scott CE, Macosko CW. Polymer 1995;36(3):461–70.
[23] Sundararaj U, Macosko CW, Rolando RJ, Chan HT. Polym Eng Sci 1992;32(24):1814–23.
[24] Bourry D, Favis BD. J Polym Sci Part B Polym Phys 1998;36(11): 1889–99.
[25] Bu W, He J. J Appl Polym Sci 1996;62(9):1445–56.
[26] Marin N, Favis BD. Polymer 2002;43(17):4723–31.
[27] Willemse RC, Posthuma de Boer A, Van Dam J, Gotsis AD. Polymer 1999;40(4):827–34.
[28] He J, Bu W, Zeng J. Polymer 1997;38(26):6347–53.
[29] Lyngaae-Jørgensen J, Rasmussen KL, Chtcherbakova EA, Utracki LA. Polym Eng Sci 1999;39(6):1060–71.
[30] Lyngaae-Jørgensen J, Kuta A, Sondergaard K, Poulsen KV. Polym Networks Blends 1993;3(1):1–13.
[31] Lyngaae-Jørgensen J. Int Polym Proc 1999;14(3):213–20.
[32] Mekhilef N, Favis BD, Carreau PJ. J Polym Sci Part B Polym Phys 1997; 35(2):293–308.
[33] Galloway JA, Montminy MD, Macosko CW. Polymer 2002;43(17): 4715–22.
[34] Vinckier I, Laun HM. Rheol Acta 1999;38(4):274–86.
[35] Heeschen WA. Polymer 1995;36(9):1835–41.
[36] Steinmann S, Gronski W, Friedrich C. Polymer 2001;42(15):6619–29.
[37] Utracki LA. J Rheol 1991;35(8):1615–37.
[38] Lacroix C, Bousmina M, Carreau PJ, Favis BD, Michel A. Polymer 1996;37(14):2939–47.
[39] Bousmina M, Muller RJ. J Rheol 1993;37(4):663–79.
[40] Friedrich C, Gleinser W, Korat E, Maier D, Weese J. J Rheol 1995;39(6): 1411–25.
[41] Vinckier I, Moldenaers P, Mewis J. J Rheol 1996;40(4):613–31.
[42] Palierne JF. Rheol Acta 1990;29(3):204–14.
[43] Weis C, Leukel J, Borkenstein K, Maier D, Gronski W, Friedrich C, et al. Polym Bull 1998;40(2–3):235–41.
[44] Mani S, Malone MF, Winter HH. J Rheol 1992;36(8):1625–50.
[45] Galloway JA, Macosko CW. Polym Eng Sci 2004;44(4):714–27.
[46] Huitric J, Medeic P, Moan M, Jarrin J. Polymer 1998;39(20): 4849–56.
[47] Steinmann S, Gronski W, Friedrich C. Rheol Acta 2002;41(1–2):77–86.
[48] Groeninckx G, Chandra S, Berghmans H, Smets G. Morphology, viscoelastic properties, and stress–strain behaviour of blends of polycarbonate of bisphenol-A (PC) and atactic polystyrene (PST). In: Cooper SL, Estes GM, editors. Multiphase polymers. Advances in chemistry series, vol. 176. Washington: ACS; 1979. p. 337–66 [chapter 18].
[49] Quintens D, Groeninckx G, Guest M, Aerts L. Polym Eng Sci 1990; 30(22):1474–83.
[50] Quintens D, Groeninckx G, Guest M, Aerts L. Polym Eng Sci 1990; 30(22):1484–90.
[51] Quintens D, Groeninckx G, Guest M, Aerts L. Polym Eng Sci 1991; 31(16):1207–14.
[52] Pötschke P, Paul DR. Macromol Symp 2003;198:69–81.
[53] Avgeropoulos GN, Weissert FC, Biddison PH, Böhm GGA. Rubber Chem Technol 1976;49:94.
[54] Nelson CJ, Avgeropoulos GN, Weissert FC, Böhm GGA. Angew Makromol Chem 1977;60/61(4):49–86.
[55] Paul DR, Barlow JW. J Macromol Sci Rev Macromol Chem 1980;C18: 109–68.
[56] Jordhamo GM, Manson JM, Sperling LH. Polym Eng Sci 1986;26(8): 517–24.
[57] Gergen WP, Lutz RG, Davidson S. Thermoplastic elastomers: a comprehensive review. In: Legge NR, Holden G, Schroeder HE, editors. Thermoplastic elastomers. Munich: Hanser Gardner Publishers; 1987. p. 507–40 [chapter 14].
[58] Miles IS, Zurek A. Polym Eng Sci 1988;28(12):796–805.
[59] Ho RM, Wu CH, Su AC. Polym Eng Sci 1990;30(9):511–8.
[60] Kitayama N, Keskkula H, Paul DR. Polymer 2000;41(22):8041–52.
[61] Everaert V, Aerts L, Groeninckx G. Polymer 1999;40(24):6627–44.
[62] Metelkin VI, Blekht VP. Coll J USSR 1984;46(3):425–9.
[63] Utracki LA. Polym Mater Sci Eng 1991;65:50–1.
[64] Galloway JA, Koester KJ, Paasch BJ, Macosko CW. Polymer 2004;45(2): 423–8.
[65] Wu S. Polym Eng Sci 1987;27(5):335–43.
[66] Boyd RH. Polymer 1985;26(3):323–47.
[67] Wunderlich B. The nature of the glass transition and its determination by thermal analysis. In: Seyler RJ, editor. Assignment of the glass transition, vol. 1249. Philadelphia: ASTM STP; 1994. p. 17–31.
[68] Frensch H, Harnischfeger P, Jungnickel BJ. Multiphase polymers: blends and ionomers. In: Utracki LA, Weiss RA, editors. ACS symposium series, vol. 395; 1989. p. 101.
[69] Ikkala OT, Holstimiettinen RM, Seppälä J. J Appl Polym Sci 1993;49(7): 1165–74.
[70] Pompe G, Pötschke P, Pionteck J. J Appl Polym Sci 2002;86(13): 3445–53.
[71] Groeninckx G, Vanneste M, Everaert V. Crystallization, morphological structure and melting of polymer blends. In: Utracki LA, editor. Polymer blends handbook, vol. 1. Dordrecht: Kluwer Academic Publishers; 2002. p. 203–94 [chapter 3].